Nonlinear Dyn (2013) 74:77–93
DOI 10.1007/s11071-013-0950-4

ORIGINAL PAPER

Numerical solution of the Schrödinger equations by using Delta-shaped basis functions

R. Mokhtari · D. Isvand · N.G. Chegini · A. Salaripanah

Received: 27 January 2013 / Accepted: 2 May 2013 / Published online: 17 May 2013

Abstract Numerical simulations of the nonlinear Schrödinger equations are studied using Delta-shaped basis functions, which recently proposed by Reutskiy. Propagation of a soliton, interaction of two solitons, birth of standing and mobile solitons and bound state solutions are simulated. Some conserved quantities are computed numerically for all cases. Then we extend application of the method to solve some coupled nonlinear Schrödinger equations. Obtained systems of ordinary differential equations are solved via the fourth- order Runge–Kutta method. Numerical solutions coincide with the exact solutions in desired machine precision and invariant quantities are conserved sensibly. Some comparisons with the methods applied in the literature are carried out.

Keywords Delta-shaped basis functions · Schrödinger equations · Fourth-order Runge–Kutta method

R. Mokhtari (✉)
Department of Mathematical Sciences, Isfahan University of Technology, Isfahan 84156-83111, Iran
e-mail: mokhtari@cc.iut.ac.ir

D. Isvand · N.G. Chegini · A. Salaripanah
Department of Mathematics, Tafresh University, Tafresh 39518-79611, Iran

D. Isvand
Instructor Training Center Technical and Vocational Researches, Abarkoh, Iran

1 Introduction

Recently, finding numerical solution of the complex nonlinear evolution equations is becoming rapidly attractive and popular [1, 2, 6–8, 10, 13, 15, 17]. One type of the famous complex nonlinear evolution equations with various and important applications in hydrodynamics, plasma physics, nonlinear optics, self-focusing in laser pulses, propagation of heat pulses in crystals, description of the dynamics of Bose–Einstein condensate at extremely low temperature, etc. is the class of Schrödinger equations [9].

The one-dimensional nonlinear Schrödinger equation (NLSE) with a central role in quantum mechanics is one of the most important equations in mathematical physics and physical chemistry with applications in many different fields such as plasma physics, nonlinear optics, water waves, particle-in-a-box, the harmonic oscillator, the hydrogen atom, the rigid rotator, and bimolecular dynamics. This equation plays the role of Newton's laws and conservation of energy in classical mechanics.

The coupled nonlinear Schrödinger equations (CNLSEs) arise in a great variety of physical situations, for example, propagation of pulses with equal mean frequencies in birefringent nonlinear fiber offers the opportunity to investigate the quasiparticle behavior soliton governed by them; see, e.g., [17] and references therein.

In the sequel, $i = \sqrt{-1}$ and $(x, t) \in (-\infty, \infty) \times (0, T)$. Considered NLSE is as follows:

$$i\frac{\partial u}{\partial t} + \frac{\partial^2 u}{\partial x^2} + q|u|^2 u = 0, \tag{1.1}$$

where q is a real parameter and $u(x, t)$, which governs weakly nonlinear, strongly dispersive, and almost monochromatic wave [23], is a complex-valued function of the spatial coordinate x and the time variable t. Usually, (1.1) is endowed with the initial condition $u(x, 0) = s(x)$ and the asymptotic boundary condition $u \to 0$ as $|x| \to \infty$.

The CNLSEs which arose in a great variety of physical situations [17] are as follows:

$$\begin{aligned} &i\left(\frac{\partial u_1}{\partial t} + \delta\frac{\partial u_1}{\partial x}\right) + \frac{1}{2}\frac{\partial^2 u_1}{\partial x^2} + \left(|u_1|^2 + e|u_2|^2\right)u_1 = 0,\\ &i\left(\frac{\partial u_2}{\partial t} - \delta\frac{\partial u_2}{\partial x}\right) + \frac{1}{2}\frac{\partial^2 u_2}{\partial x^2} + \left(e|u_1|^2 + |u_2|^2\right)u_2 = 0, \end{aligned} \tag{1.2}$$

where e is the cross phase modulation coefficient, δ is the normalized strength of the linear birefringence, and u_1 and u_2 are the wave amplitude in two polarizations.

The strong coupled nonlinear Schrödinger equations (SCNLSEs) which considered here are as follows:

$$\begin{aligned} &i\frac{\partial u_1}{\partial t} + \beta\frac{\partial^2 u_1}{\partial x^2} + \left(\alpha_1|u_1|^2 + (\alpha_1 + 2\alpha_2)|u_2|^2\right)u_1\\ &\quad + \gamma u_1 + \Gamma u_2 = 0,\\ &i\frac{\partial u_2}{\partial t} + \beta\frac{\partial^2 u_2}{\partial x^2} + \left(\alpha_1|u_2|^2 + (\alpha_1 + 2\alpha_2)|u_1|^2\right)u_2\\ &\quad + \gamma u_1 + \Gamma u_1 = 0, \end{aligned} \tag{1.3}$$

where the linear coupling parameter Γ accounts for effects that arise from the twisting of the fiber and elliptic deformation of a fiber. It is also referred to the linear birefringence or relative propagation constant. The term proportional to α_1 describes the self-focusing of a signal for pulses in birefringent media. The parameter β describes the group velocity dispersion, and $(\alpha_1 + 2\alpha_2)$ is the cross phase modulation. Finally, the term γ appears as constant ambient potential called normalized birefringence.

Equations (1.2) and (1.3) are usually equipped with the following initial conditions:

$$u_1(x, 0) = s_1(x), \qquad u_2(x, 0) = s_2(x), \qquad -\infty < x < \infty,$$

and the following asymptotic boundary conditions

$$u_1, u_2 \to 0, \quad |x| \to \infty.$$

In this study, we aim to solve numerically NLSE (1.1), CNLSEs (1.2), and SCNLSEs (1.3) by using a boundary method of Treffz-type newly developed by Reutskiy et al. [18–21]. When this method applies in a collocation regime, it can be considered as a meshless collocation method similar to the radial basis functions (RBFs) collocation method, which has shown to provide a truly meshless computational approach for solving various partial differential equations (PDEs); see, e.g., [14, 16] and references therein. Such methods have advantage in comparing with most traditional mesh-dependent methods such as finite element and finite difference method since mesh construction is not a trivial work especially for nonlinear, moving boundary, and multidimensional problems [5].

The rest of the paper is organized as follows. In Sect. 2, we describe briefly the Delta-shaped basis functions. Without taking details into account, construction of a semi-discrete method based on the Delta-shaped basis functions is described in Sect. 3. Section 4 is devoted to the numerical results. Section 5 is a brief conclusion.

2 Delta-shaped basis functions

New delta-shaped basis function derived by Reutskiy from the Fourier series of the Dirac-delta function can be applied to successfully simulate a set of scattered data in regular or irregular domains [5, 18–21]. In the sequel, we describe briefly these functions. Let $(\varphi_n(x), \lambda_n)$ be a solution of the following Sturm–Liouville eigenvalue problem

$$\begin{cases} -\dfrac{d^2\varphi}{dx^2} = \lambda\varphi, \quad x \in (-1, 1),\\ \varphi(-1) = \varphi(1) = 0. \end{cases} \tag{2.1}$$

Obviously, $\lambda_n = \frac{n\pi}{2}$, $\varphi_n(x) = \sin(n\pi\frac{x+1}{2})$, and furthermore

$$\int_{-1}^{1} \varphi_m(x)\varphi_n(x)\,dx = \delta_{mn} = \begin{cases} 1, & m = n, \\ 0, & m \neq n. \end{cases}$$

In other words, eigenfunctions $\{\varphi_n(x)\}_{n=1}^{\infty}$ form an orthogonal system on [-1,1] and the Dirac's delta function can be formally written as follows:

$$\delta(x-\xi) = \sum_{n=1}^{\infty} \varphi_n(\xi)\varphi_n(x). \tag{2.2}$$

Since this series diverges at any point in the interval $[-1, 1]$, using some kinds of regularization techniques such as Lanczos or Riesz or Abel [19], a smooth delta-shaped function, $I_{M,\chi}(x,\xi)$, can be obtained through the formal series expansion (2.2). We consider here the Riesz regularization technique and, therefore, the regularized delta-shaped functions have the form

$$I_{M,\chi}(x,\xi) = \sum_{n=1}^{M} \left(1 - \frac{n^2}{(M+1)^2}\right)^{\chi} \varphi_n(\xi)\varphi_n(x). \tag{2.3}$$

Here, χ plays the role of regularizing and M plays the role of scaling. The support of the basis function decreases as M increases. The parameters M and χ which can be known shape parameters (because of their close relation with the properties of the functions) should be taken in coupling. It must be pointed out that the optimal choice of these shape parameters is an open problem and can be dealt with experimentally. In general, choosing $\chi = 4, 6, 8, 12, 14, 16, 18$ for $M = 10, 20, 30, 40, 50, 80, 100$ is found to be close to the optimal one. More details can be found in [18, 21].

3 Construction of the method

In order to approximate solution to (1.1), we assume that f and g are real and imaginary parts of u, respectively, i.e.,

$$u(x,t) = f(x,t) + ig(x,t). \tag{3.1}$$

Substituting (3.1) into (1.1) leads to the following coupled real partial differential equations:

$$\begin{cases} g_t = f_{xx} + q\left(f^2+g^2\right)f, \\ f_t = -g_{xx} - q\left(f^2+g^2\right)g. \end{cases} \tag{3.2}$$

For solving (1.1) on the interval $[a,b]$, artificial boundary conditions $u(a,t) = 0$ and $u(b,t) = 0$ are needed to model the physical boundary condition. Therefore, system (3.2) must be equipped with the following boundary conditions:

$$f(a,t) = f(b,t) = 0 = g(a,t) = g(b,t), \quad t \in [0,T].$$

Then, we choose some center points

$$\xi_1 < \xi_2 < \cdots < \xi_N,$$

in the interval $[a,b]$ and approximate f and g as follows:

$$\begin{cases} f(x,t) \simeq \sum_{j=1}^{N} f_j(t) I_{M,\chi}(x,\xi_j), \\ g(x,t) \simeq \sum_{j=1}^{N} g_j(t) I_{M,\chi}(x,\xi_j). \end{cases} \tag{3.3}$$

By choosing some collocation points,

$$a = x_1 < x_2 < \cdots < x_N = b,$$

(often equidistant with step size h) substituting (3.3) into (3.2) and imposing boundary conditions, we get a system of ordinary differential equations which can be solved with the aid of the classical Runge–Kutta method of order four (RK4).

It must be pointed out that center points and collocation points are different but for ease of computation it is better to be identical.

We end this section by stating the following useful proposition which proved by Hon et al. [5].

Proposition 3.1 *The coefficient matrix*

$$A = \left[I_{M,\chi}(x_k,\xi_j)\right]_{N\times N}$$

is positive definite if $M \geq N$.

4 Numerical results

4.1 Numerical tests of NLSE

Accuracy of the numerical results are measured by using the following L_∞ error norm

$$E_\infty = \left\|u^n - U^n\right\|_\infty = \max_j \left|u_j^n - U_j^n\right|. \tag{4.1}$$

where u^n and U^n denote the exact and numerical solution at nth time level, respectively. The reliable soliton solutions of Eq. (1.1) must keep some conservation laws [24]. The following two conserved quantities are considered here:

$$C_1 = \int_a^b |u|^2\,dx \approx h\sum_{j=0}^{N}\left|U_j^n\right|^2, \tag{4.2}$$

$$C_2 = \int_a^b \left[|u_x|^2 - \frac{1}{2}q|u|^4\right]dx \approx h\sum_{j=1}^{N}\left(\left|(U_x)_j^n\right|^2 - \frac{1}{2}q\left|U_j^n\right|^4\right). \tag{4.3}$$

Relative changes of invariants are defined as $EC_1 = \frac{C_1-C_1^0}{C_1^0}$ and $EC_2 = \frac{C_2-C_2^0}{C_2^0}$ where C_1^0 and C_2^0 are the values of the conserved quantities C_1 and C_2 at time $t = 0$, respectively.

4.1.1 Motion of single soliton

Equation (1.1) has been used to model a number of physical situations involving nonlinearity and dispersion. When a certain balance is reached between nonlinearity and dispersion, solitons are formed. This is simply illustrated by the single soliton solution of the equation as follows:

$$u(x,t) = \alpha\left(\frac{2}{q}\right)^{1/2}\exp\left(i\left\{\frac{1}{2}cx - \frac{1}{4}\left(c^2-\alpha^2\right)t\right\}\right) \times \operatorname{sech}\left(\alpha(x-ct)\right), \tag{4.4}$$

where c represents the speed of the soliton whose magnitude depends on α, which determines its amplitude. Parameters $q = 2$, $c = 4$, $\alpha = 1$ and solution interval $-20 \le x \le 20$ are chosen to coincide with earlier works so that comparison of results can be done. We establish the initial condition and boundary conditions from the exact solution (4.4). Analytical values of conserved quantities are $C_1 = 2$ and $C_2 = 7.33333333333334$. In Table 1, L_∞-error norm and relative errors of conserved quantities are shown for various time and space step size.

For $M = 4000$ and $\chi = 1200$, graph of the travelling soliton is presented in Figs. 1, 2, 3 and 4 at different times $t = 0.0$, $t = 1.0$ and $t = 2.5$ in which the real and imaginary components and the modules are displayed. Plot of the error at time $t = 1.0$ for the parameters $M = 4000$, $\chi = 1200$, $h = 0.125$ and $\Delta t = 0.0025$ is shown in Fig. 5. Results are reasonably comparable with the other numerical method [10].

For obtaining experimental optimal values of M and χ, one can repeat computation once by changing χ for fixed M and then by changing M for fixed χ. Results depicted in Table 2 imply that this problem is not a problem of extreme sensitivity with respect to choosing M and χ.

4.1.2 Interaction of two solitons

Interaction of two positive solitary waves is studied by using the initial condition

$$u(x,0) = u_1(x,0) + u_2(x,0). \tag{4.5}$$

where

$$u_j(x,0) = \alpha_j\left(\frac{2}{q}\right)^{1/2}\exp\left(i\left\{\frac{1}{2}c_j(x-x_j)\right\}\right) \times \operatorname{sech}\left(\alpha_j(x-x_j)\right), \quad j = 1,2. \tag{4.6}$$

We choose the parameters $q = 2$, $h = 0.125$, $\Delta t = 0.0025$, $\alpha_1 = 1.0$, $\alpha_2 = 0.1$, $x_1 = -10$, $x_2 = 10$, $c_1 = 4$, $c_2 = 10$, and $-20 \le x \le 20$. These parameters give solitons with the equal amplitudes 9.999999972506763e−001 occurring at $x_1 = -10$ and $x_2 = 10$, respectively, and both of them have the velocity of 4 but move in opposite direction, collide and separate. The simulation of interaction is shown at different times in Fig. 6. Results are in good agreement with other numerical methods [2, 4, 10].

Conserved quantities and amplitudes and peak positions of both solitons at various times and comparison of conserved quantities and their relative changes with some earlier works are seen at Fig. 7 and Tables 3 and 4, respectively. The conservation laws are satisfied up to time $t = 5.0$ with a greater degree of accuracy. C_1 and C_2 remain the same to eight digits at time $t = 5.0$, that are better than results in [10].

4.1.3 Maxwellian initial condition

According to the theory, if $\int_{-\infty}^{\infty} u(x,0)\,dx \ge \pi$, a soliton is generated, or else it fades out [3]. This is studied in the paper using the Maxwellian initial condition, given by [4],

$$u(x,0) = A\exp\left(-x^2\right), \tag{4.7}$$

Table 1 Comparison of single soliton solution of Eq. (1.1) at time $t = 1$ for $M = 4000$

Method	χ	h	Δt	$E_\infty \times 10^5$	EC_1	EC_2
Delda-shaped	5000	0.4	0.01	12	−4.536e−008	−4.407e−008
Delda-shaped	2300	0.3125	0.025	1.5	−4.379e−006	−1.214e−005
Delda-shaped	7300	0.3125	0.01	0.021	−4.467e−008	−1.249e−007
Delda-shaped	7300	0.3125	0.02	2.3	−1.438e−006	−3.992e−006
Delda-shaped	1200	0.125	0.0025	0.01	1.758e−011	2.401e−010
Delda-shaped	1200	0.125	0.001	0.01	6.125e−011	3.615e−010
Delda-shaped	100	0.05	0.000625	0.01	−5.698e−013	−6.162e−013
CDQ [10]		0.3125	0.01	5.6	4.380e−06	1.214e−05
CDQ [10]		0.3125	0.01	0.2	4.512e−08	1.253e−07
CDQ [10]		0.125	0.01	0.2	4.412e−011	1.226e−010
CDQ [10]		0.125	0.01	0.02	4.541e−013	1.266e−012
PDQ [11]		0.1	0.0025	0.02	−5.222e−011	2.931e−09
PDQ [11]		0.3125	0.02	2.53	−1.440e−06	−3.942e−06
B-spline Galerkin [2]		0.05	0.005	30	0.0000000	0.0000006
B-spline Galerkin [2]		0.3125	0.020	200	0.0000066	0.0003417
B-spline Col [4]		0.05	0.005	800	0.00000	0.00000
B-spline Col [4]		0.03	0.005	200	0.00000	0.00000
Explicit [22]		0.05	0.000625	600	0.00000	60.0055
Implicit/explicit [22]		0.05	0.001	600	0.00309	0.01205
Implicit (C-N) [22]		0.05	0.005	600	0.00001	0.00557
Hopscotch [22]		0.08	0.002	500	0.00003	0.01407
Split-step Fourier [22]		0.3125	0.020	500	0.00000	0.00005
A-L Local [22]		0.06	0.0164	600	0.00004	0.00797
A-L Global [22]		0.05	0.040	600	0.00003	0.00550
Pseudospectral [22]		0.3125	0.00026	500	0.00001	0.00003

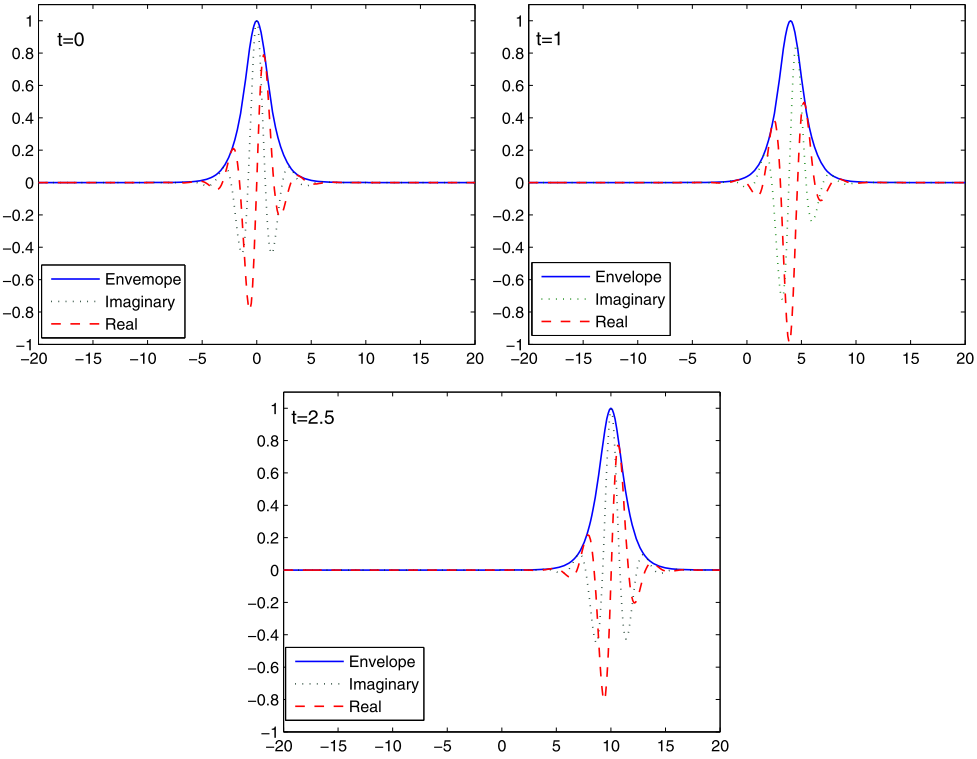

Fig. 1 Single soliton with real and imaginary components and the modules at different times 0, 1, and 2.5

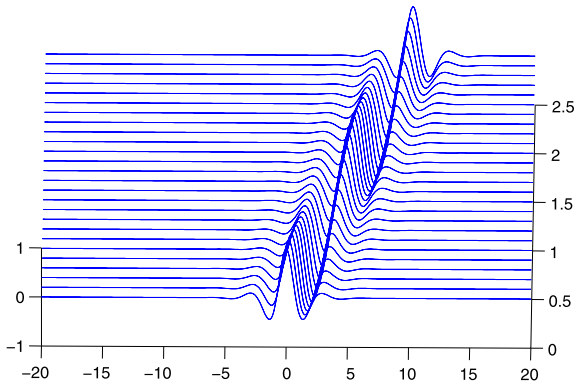

Fig. 2 Imaginary part of single soliton at different times

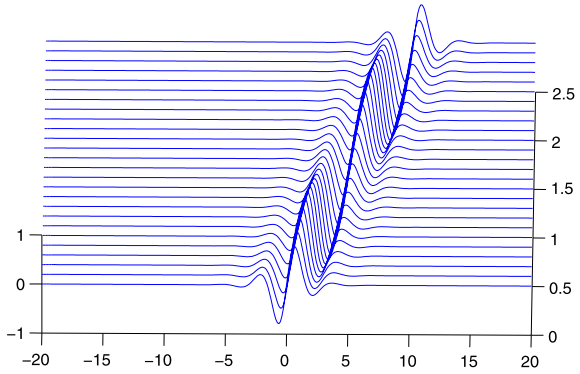

Fig. 3 Real part of single soliton at different times

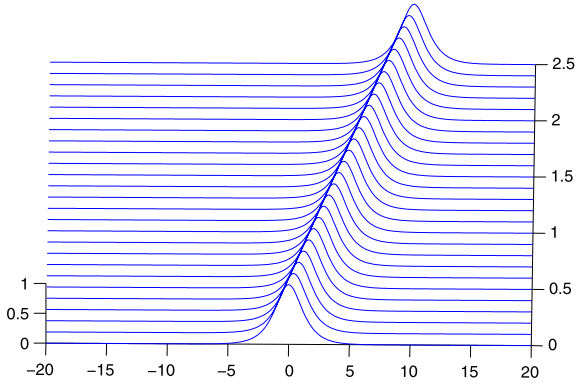

Fig. 4 Modules of single soliton at different times

where $h = 0.15$, $\Delta t = 0.002$ and $q = 2$ for the domain $-45 \leq x \leq 45$. Numerical experiment of the birth of soliton is carried out for the values $A = 1$ and 1.78. The program is run until the time $t = 6$ to observe the development of the soliton. Figure 8 presents the birth of standing soliton with $A = 1.78$ while the solution

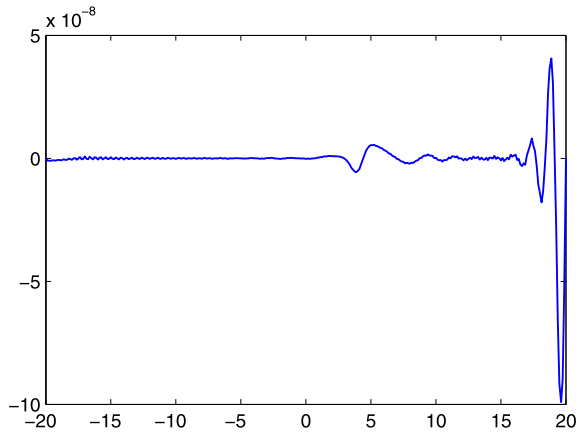

Fig. 5 Plot of error at time $t = 1$ with $M = 4000$, $\chi = 1200$, $h = 0.01$ and $\Delta t = 0.0025$

Table 2 Investigating error of single soliton solution of Eq. (1.1) for $h = 0.125$ and $dt = 0.001$ up to time $t = 1$ for different values of M and χ

$M = 1000$		$M = 2000$		$\chi = 200$	
χ	E_∞	χ	E_∞	M	E_∞
10	5.17e−005	40	3.21e−002	1510	5.71e−004
20	1.05e−007	50	4.32e−003	1520	2.86e−005
30	1.02e−007	60	5.36e−004	1530	1.33e−006
40	1.01e−007	80	7.32e−006	1540	1.75e−007
50	1.01e−007	100	1.04e−007	1550	1.02e−007
60	1.01e−007	150	1.02e−007	1600	1.01e−007
70	1.01e−007	200	1.01e−007	1800	1.01e−007
80	6.43e−006	250	1.01e−007	2000	1.01e−007
81	8.99e−005	300	1.01e−007	2500	1.02e−007
83	1.20e−003	350	2.87e−006	3000	3.37e−006
86	8.93e+000	360	1.24e−003	3200	3.26e−005

decays away with value $A = 1$ as shown in Fig. 9. Maximas of the solutions are drawn in Fig. 10 from which evolution of soliton of magnitude of about 4 and dissolution can visualized clearly. Thus, the theory is verified that if $A = 1.78 > \sqrt{\pi} = 1.7725$, a soliton is produced, so with choice of the less than $A < \sqrt{\pi}$ initial soliton decays away. Conserved quantities for both cases are graphed in Figs. 11 and 12. Using the Maxwellian initial condition (4.7), analytical conserved quantities can be computed as following:

$$C_1 = A^2\sqrt{\pi/2} \quad \text{and} \quad C_2 = \frac{1}{4}A^2\left(2\sqrt{2} - qA^2\right)\sqrt{\pi},$$

and results of those quantities and their relative errors are recorded in Table 5. Consequently, conserved

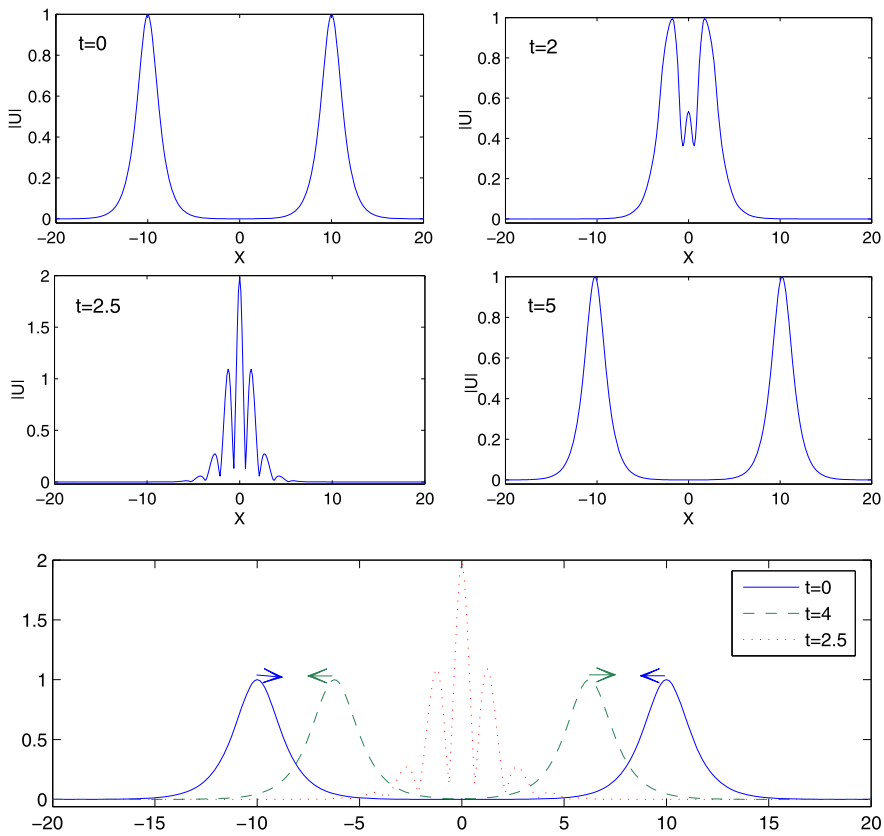

Fig. 6 Interaction of two solitons at different times $t = 0, 2, 2.5, 5$ with $M = 4000$, $\chi = 500$, $h = 0.125$ and $\Delta t = 0.0025$

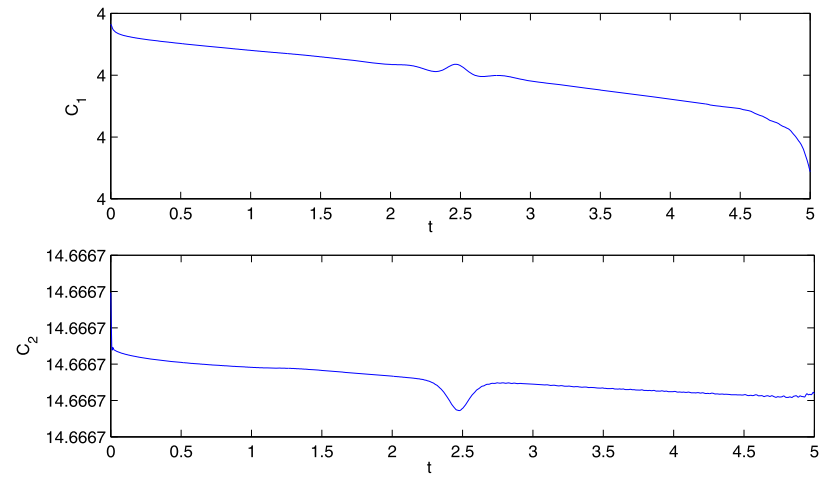

Fig. 7 Values of C_1 and C_2 for interaction of two solitons with $M = 4000$, $\chi = 500$, $h = 0.125$ and $\Delta t = 0.0025$

quantities obtained using numerical method preserved satisfactorily well.

4.1.4 Birth of mobile soliton

The birth of the mobile soliton is studied using the initial condition

$$u(x, 0) = A \exp\left(-x^2 + 2ix\right), \tag{4.8}$$

where $h = 0.125$ and $\Delta t = 0.001$ over the domain $[-30, 80]$. Simulation is studied with values $A = 1$ and $A = 1.78$ to see solutions until time $t = 6.0$. Mobile soliton of amplitude 4 is produced with $A = 1.78$ and the formation of soliton can be observed form the Fig. 13. Once again solution is faded out with $A = 1$ and is graphed in Fig. 14. Maximas of two solutions and conserved quantities are depicted in Figs. 15

Table 3 Values of C_1 and C_2 for interaction of two solitons with $M = 4000$, $\chi = 500$, $h = 0.125$ and $\Delta t = 0.0025$

t	C_1	C_2	Soliton 1		Soliton 2	
			Amplitude and peak position		Amplitude and peak position	
0	3.999999991	14.6666669	0.9999999972506763	−10	0.9999999972506763	10
0.5	3.999999991	14.6666668	0.9999946921173225	−8	0.9999946921173085	8
1	3.999999990	14.6666668	1.000000639378599	−6	1.000000639378603	6
1.5	3.999999990	14.6666668	0.9994579125790593	−4	0.9994579125791129	4
2	3.999999990	14.6666668	0.9948743169607603	−1.75	0.9948743169608429	1.75
2.5	3.999999990	14.6666668	1.984567952311632	0	1.984567952311632	0
3	3.999999990	14.6666668	0.9740967405227943	2.25	0.9740967405230238	−2.25
3.5	3.999999990	14.6666668	0.9997326716422408	4.25	0.9997326716425774	−4.25
4	3.999999990	14.6666668	0.9996466059149936	6.25	0.9996466059154411	−6.25
4.5	3.999999989	14.6666668	0.9996448724566495	8.25	0.9996448724571159	−8.25
5	3.999999988	14.6666667	0.9996414215448909	10.25	0.9996414215453822	−10.25

Table 4 Comparison of two soliton simulations with some earlier results for $M = 4000$

Method	χ	h	Δt	Time	EC_1	EC_2
Delda-shaped	2500	0.2	0.005	2.5	−2.7e−009	−1.3e−006
Delda-shaped	500	0.125	0.001	2.5	1.1e−010	−9.8e−009
Delda-shaped	500	0.125	0.001	2.5	−1.4e−011	−7.9e−009
Delda-shaped	800	0.13	0.0036	2.5	−6.0e−010	−1.8e−008
Delda-shaped	4000	0.625	0.005	2.5	−2.3e−005	4.6e−003
Delda-shaped	2300	0.3125	0.01	3	−1.4e−007	−3.9e−007
Delda-shaped	2300	0.3125	0.005	3	−4.3e−009	−3.0e−008
Delda-shaped	2300	0.25	0.01	3	−1.3e−007	−3.7e−007
Delda-shaped	500	0.125	0.0025	3	−2.3e−010	−8.6e−009
CDQ [10]		0.25	0.010	2.5	−1.0e−007	−6.1e−006
CDQ [10]		0.25	0.005	2.5	−3.0e−009	−5.8e−006
CDQ [10]		0.20	0.005	2.5	−3.0e−009	−1.6e−007
PDQ [11]		0.25	0.010	2.5	−6.0e−008	−4.4e−006
PDQ [11]		0.25	0.005	2.5	4.1e−008	−4.1e−006
PDQ [11]		0.20	0.005	2.5	3.1e−009	−5.2e−007
Explicit [22]		0.13	0.0036	2.5	0.00000	0.0066
Split-step Fourier [22]		0.625	0.005	2.5	0.00071	0.036

and 16, respectively. Conserved quantities and their relative errors are presented in Table 6. Both invariants for this simulation are conserved reasonably well.

4.1.5 Bound state of solitons

For the soliton solutions of the Schrödinger equation, the speed and amplitude can be selected separately. This allows solitons to move at same speeds all the time interacting with the other one. Precise results are obtained by Miles [12] by using initial condition

$$u(x, 0) = \operatorname{sech}(x), \tag{4.9}$$

which produces a bound state of λ solutions if

$$q = 2\lambda^2, \quad \lambda = 1, 2, \ldots.$$

However, the solution does not have usable form if $\lambda \geq 3$. Numerical studies are conducted for bound state of solitons with the initial conditions using the parameters $q = 2, 8, 18, 32$. Solution of this problem includes extremely large space and time gradients thus producing a numerical method to model these behavior have quite importance in terms of the numerical analysts. Conserved quantities with initial condition

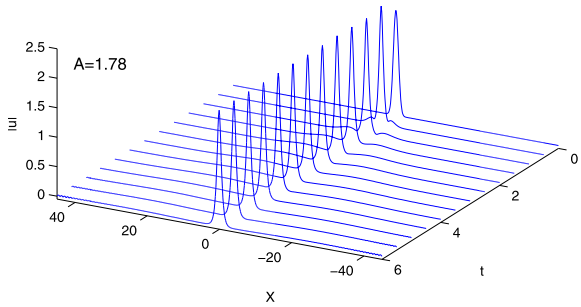

Fig. 8 Maxwellian with $A = 1.78$, $h = 0.15$, $\Delta t = 0.002$, $M = 4000$ and $\chi = 500$

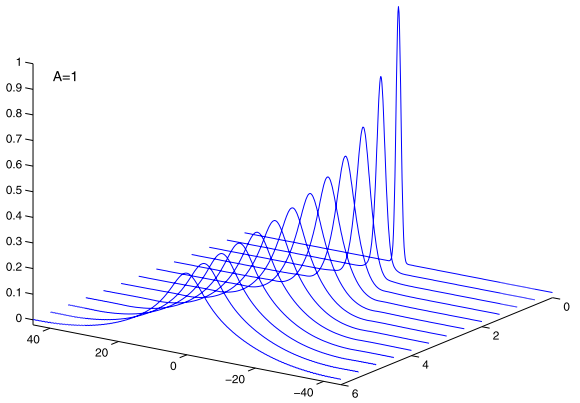

Fig. 9 Maxwellian with $A = 1$, $h = 0.15$, $\Delta t = 0.002$, $M = 4000$ and $\chi = 500$

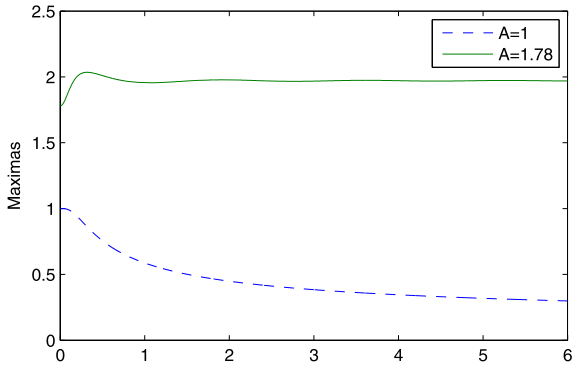

Fig. 10 Maximas, amplitude of wave for $A = 1$ and $A = 1.78$ with $h = 0.15$, $\Delta t = 0.002$, $M = 4000$, and $\chi = 500$

(4.9) can be computed analytically by

$$C_1 = 2, \qquad C_2 = \frac{2}{3}(1-q). \tag{4.10}$$

With considering rounding errors and computational costs, some numerical methods can be applied in practice to conserve quantities to a fixed number of digits. Parameters $h = 0.1$, $\Delta t = 0.0005$, $M = 4000$, $\chi = 700$, and $q = 18,\ 32$ over a region $-20 \le x \le 20$ are used for the sake of the comparison with studies. When $q = 18$, graphs are depicted in Fig. 17 at early times of simulation in which shapes of 3 bound solitons are in complete agreement with the papers [4, 10]. The graph of modules of the numerical solution from the discrete set of data is also produced successfully for $q = 32$ shown in Fig. 18. Both invariants for both cases remain almost constant and reflect the satisfactory as illustrated in Table 7 with $q = 18$, C_1 and C_2 are converged up to 6 and 5 digits, respectively, at time $t = 5$. Situation deteriorated little with $q = 32$ since changes of C_1 and C_2 are happened at fourth digit.

4.2 Numerical tests of CNLSEs

Consider the CNLS equations (1.2), and let

$$\begin{aligned} u_1(x,t) &= f_1(x,t) + i g_1(x,t), \\ u_2(x,t) &= f_2(x,t) + i g_2(x,t), \end{aligned} \tag{4.11}$$

where $f_j(x,t)$ and $g_j(x,t)$ for $j = 1, 2$ are the real functions. Substituting Eq. (4.11) into Eq. (1.2) leads to the associated two coupled pair of real partial differential equations

$$\begin{aligned} \frac{\partial f_1}{\partial t} &= -\delta \frac{\partial f_1}{\partial x} - \frac{1}{2}\frac{\partial^2 g_1}{\partial x^2} - p_1 g_1, \\ \frac{\partial g_1}{\partial t} &= -\delta \frac{\partial g_1}{\partial x} + \frac{1}{2}\frac{\partial^2 f_1}{\partial x^2} + p_1 f_1, \\ \frac{\partial f_2}{\partial t} &= \delta \frac{\partial f_2}{\partial x} - \frac{1}{2}\frac{\partial^2 g_2}{\partial x^2} - p_2 g_2, \\ \frac{\partial g_2}{\partial t} &= \delta \frac{\partial g_2}{\partial x} + \frac{1}{2}\frac{\partial^2 f_2}{\partial x^2} + p_2 g_2, \end{aligned} \tag{4.12}$$

where $p_1 = (f_1^2 + g_1^2 + e(f_2^2 + g_2^2))$ and $p_2 = (e(f_1^2 + g_1^2) + f_2^2 + g_2^2)$. For solving (1.2) on the interval $[a, b]$, artificial boundary conditions $u_j(a,t) = 0$ and $u_j(b,t) = 0$ for $j = 1, 2$ are needed to model the physical boundary condition. Therefore, system (4.12) must be equipped with the following boundary conditions:

$$\begin{aligned} f_1(a,t) = g_1(a,t) = f_2(a,t) = g_2(a,t) = 0, \\ f_1(b,t) = g_1(b,t) = f_2(b,t) = g_2(b,t) = 0, \end{aligned}$$

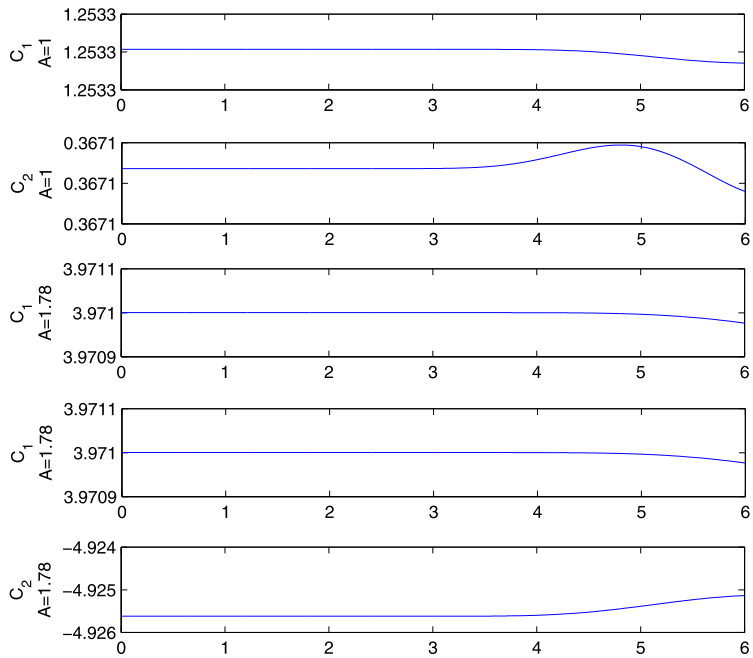

Fig. 11 Conservation quantity for $A = 1$ and $A = 1.78$ with $h = 0.15$, $\Delta t = 0.002$, $M = 4000$, and $\chi = 500$

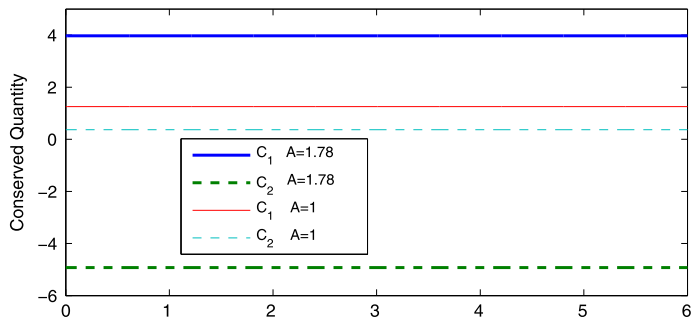

Fig. 12 Conservation quantity for $A = 1$ and $A = 1.78$ with $h = 0.15$, $\Delta t = 0.002$, $M = 4000$, and $\chi = 500$

Table 5 Error of conserved quantities for Maxwellian with parameters $M = 4000$, $\chi = 500$, $h = 0.15$ and $\Delta t = 0.002$

t	EC_1	EC_2
$A = 1$		
1	−5.9e−011	−8.2e−010
2	−9.6e−011	−1.1e−009
3	−6.0e−011	1.5e−007
4	−1.5e−008	1.2e−005
5	−2.6e−007	2.9e−005
6	−5.8e−007	−3.1e−005
$A = 1.78$		
1	3.5e−011	4.8e−010
2	3.8e−011	6.9e−010
3	1.1e−010	−6.4e−009
4	−2.0e−008	−4.5e−006
5	−9.2e−007	−4.7e−005
6	−6.0e−006	−9.8e−005

where $t \in [0, T]$. Then we choose some center points

$$\xi_1 < \xi_2 < \cdots < \xi_N,$$

in the interval $[a, b]$ and approximate f_1, f_2, g_1 and g_2 as follows:

$$\begin{cases} f_1(x,t) \simeq \sum_{j=1}^{N} f_{1j}(t) I_{M,\chi}(x, \xi_j), \\ f_2(x,t) \simeq \sum_{j=1}^{N} f_{2j}(t) I_{M,\chi}(x, \xi_j), \\ g_1(x,t) \simeq \sum_{j=1}^{N} g_{1j}(t) I_{M,\chi}(x, \xi_j), \\ g_2(x,t) \simeq \sum_{j=1}^{N} g_{2j}(t) I_{M,\chi}(x, \xi_j). \end{cases} \tag{4.13}$$

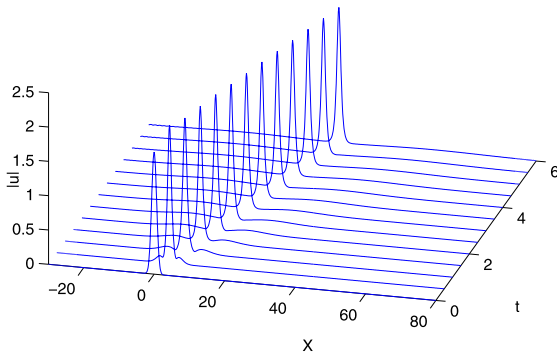

Fig. 13 Birth of a soliton for $A = 1.78$, $h = 0.125$, $\Delta t = 0.001$, $M = 4000$, $\chi = 150$

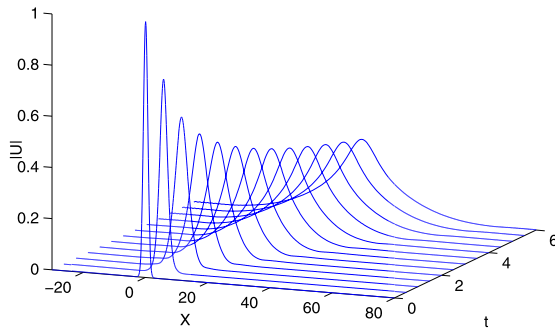

Fig. 14 Birth of a soliton for $A = 1$, $h = 0.125$, $\Delta t = 0.001$, $M = 4000$, $\chi = 150$

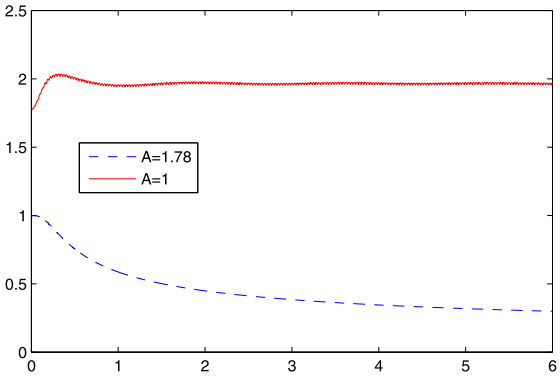

Fig. 15 Amplitude of birth of a soliton for $h = 0.125$, $\Delta t = 0.001$, $M = 4000$, $\chi = 150$

Assuming that N collocation points are distributed uniformly in the domain $[a, b]$ as $a = x_1 < \cdots < x_N = b$ and substituting (4.13) into (4.12) and imposing boundary conditions, a system of ordinary differential equations will be obtained which can be solved with the aid of RK4. In order to obtain a reliable solution, discrete conservation quantities are important features in computing smooth soliton solutions of the CNLS equations. The mass, momentum, and energy conservation quantities of the solution to Eq. (1.2) are computed numerically by employing the composite rectangle rules as follows:

$$I_1 = \int_{\infty}^{\infty} |u_1|^2\,dx \approx h\sum_{j=0}^{N} |u_1^j|^2,$$

$$I_2 = \int_{\infty}^{\infty} |u_2|^2\,dx \approx h\sum_{j=0}^{N} |u_2^j|^2,$$

$$I_3 = \int_{\infty}^{\infty} i\sum_{l=1}^{2}(\overline{u}_l u_{lx} - \overline{u}_{lx} u_l)\,dx$$

$$\approx h\sum_{j=0}^{N} i\left((\overline{u}_1^j u_{1x}^j - \overline{u}_{1x}^j u_1^j) + (\overline{u}_2^j u_{2x}^j - \overline{u}_{2x}^j u_2^j)\right),$$

$$I_4 = \int_{\infty}^{\infty}\left(\frac{1}{2}\sum_{l=1}^{2}|u_{lx}|^2 - \frac{1}{2}\sum_{l=1}^{2}|u_l|^4 - e|u_1|^2|u_2|^2\right)dx$$

$$\approx h\sum_{j=1}^{N}\left(\frac{1}{2}\sum_{l=1}^{2}|u_{lx}^j|^2 - \frac{1}{2}\sum_{l=1}^{2}|u_l^j|^4 - e|u_1^j|^2|u_2^j|^2\right).$$

For $k = 1, 2, 3, 4$, the relative error EI_k is defined as $EI_k = \frac{I_k - I_k^0}{I_k^0}$ where I_k^0 is the value of conserved quantity I_k at time $t = 0$. Furthermore, the accuracy of the method is measured by using the L_∞ error norm defined by

$$E_\infty = \max_{1\le x\le N}\left(|u_1(x_j, t)| - |f_{1j} + ig_{1j}|\right).$$

The exact solution of Eq. (1.2) is

$$u_1(x,t) = \sqrt{\frac{2\alpha}{1+e}}\,\mathrm{sech}\left(\sqrt{2\alpha}(x - \nu t)\right) \times \exp\left(i(\nu - \delta)x - \left(\frac{\nu^2 - \delta^2}{2} - \alpha\right)t\right),$$

$$u_2(x,t) = \sqrt{\frac{2\alpha}{1+e}}\,\mathrm{sech}\left(\sqrt{2\alpha}(x - \nu t)\right) \times \exp\left(i(\nu + \delta)x - \left(\frac{\nu^2 - \delta^2}{2} - \alpha\right)t\right),$$

where α and ν are real parameters. Consider the CNLS equations (1.2), subject to the initial conditions

$$u_1(x,0) = \sqrt{\frac{2\alpha}{1+e}}\,\mathrm{sech}\left(\sqrt{2\alpha}x\right)\exp\left(i(\nu - \delta)x\right),$$
$$u_2(x,0) = \sqrt{\frac{2\alpha}{1+e}}\,\mathrm{sech}\left(\sqrt{2\alpha}x\right)\exp\left(i(\nu + \delta)x\right), \tag{4.14}$$

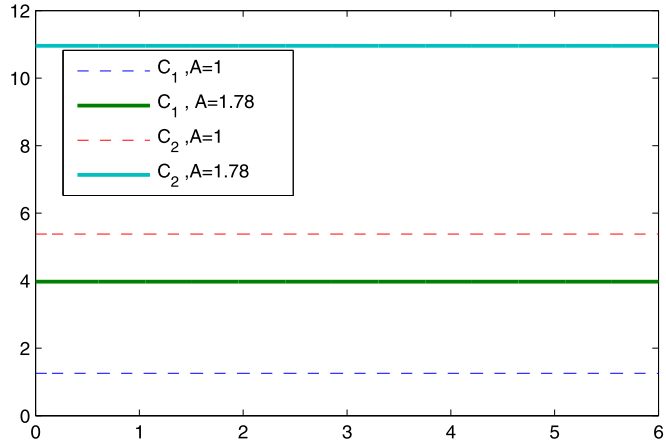

Fig. 16 Birth of soliton conservation quantity for $h = 0.125$, $\Delta t = 0.001$, $M = 4000$, $\chi = 150$

Table 6 Error of birth of a mobile soliton with $A = 1$ and $A = 1.78$, $h = 0.125$, $\Delta t = 0.001$, $M = 4000$, $\chi = 150$ on domain $[-30, 80]$

t	EC_1	EC_2
$A = 1.78$		
1	−4.1e−011	−2.6e−010
2	−6.5e−011	−4.6e−010
3	−1.6e−010	−1.6e−010
4	−1.5e−008	5.4e−008
5	−1.7e−007	1.8e−007
6	−1.3e−006	−3.6e−006
$A = 1$		
1	−1.1e−011	−7.7e−011
2	−1.9e−011	−1.3e−010
3	−4.2e−010	1.5e−009
4	−1.5e−008	6.8e−009
5	−9.3e−008	−5.5e−008
6	−4.5e−007	−1.8e−006

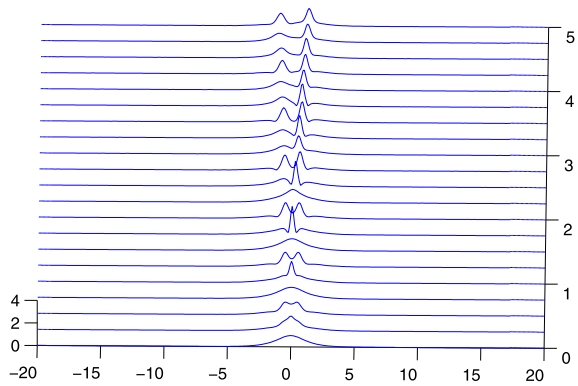

Fig. 17 Bound state for $\lambda = 3$

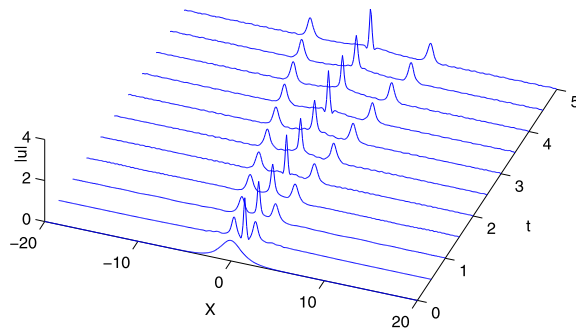

Fig. 18 Bound state for $\lambda = 4$

Table 7 Error of bound state solitons for $h = 0.1$, $\Delta t = 0.0005$, $M = 4000$ and $\chi = 700$ over a region $-20 \le x \le 20$

t	EC_1	EC_2
$\lambda = 3$		
1	2.3e−009	1.8e−005
2	−2.2e−007	1.0e−006
3	−9.9e−007	−2.8e−006
4	−1.7e−006	9.0e−006
5	−2.4e−006	1.1e−005
$\lambda = 4$		
1	4.7e−006	−2.5e−004
2	−3.1e−005	9.0e−004
3	−3.7e−005	−6.8e−004
4	−4.7e−005	−4.8e−004
5	−5.2e−005	−7.8e−004

where α, e, and ν are constants [7, 17]. By setting

$$a = -20, \quad b = 60, \quad \nu = 1, \quad \alpha = 1, \quad e = 1, \quad \delta = 0, \tag{4.15}$$

Table 8 Error of a single soliton solution at $t = 12$ for $M = 4000$

Method	χ	h	Δt	E_∞
$\delta = 0$				
Delda-shaped	1200	0.3125	0.025	4.5e−005
Delda-shaped	1200	0.3125	0.01	4.7e−005
Delda-shaped	300	0.125	0.002	1.8e−011
Delda-shaped	400	0.2	0.002	6.3e−007
Delda-shaped	600	0.2	0.002	1.5e−008
CDQ [15]		0.3125	0.025	4.8e−005
CDQ [15]		0.3125	0.01	4.8e−005
CDQ [15]		0.125	0.008	3.8e−009
DRK4 [6]		0.1	0.008	2.0e−004
DIMPR [6]		0.1	0.008	2.3e−004
GM [7]		0.1	0.01	3.6e−002
$\delta = 0.5$				
Delda-shaped	300	0.3125	0.04	4.0e−005
Delda-shaped	400	0.2	0.02	1.9e−007
Delda-shaped	400	0.2	0.002	1.3e−008
Delda-shaped	400	0.125	0.002	1.2e−008
CDQ [15]		0.3125	0.04	5.0e−005
CD [8]		0.2	0.04	2.8e−003
CSC [17]		0.2	0.04	3.5e−004

Table 9 Relative errors of conserved quantities for a single soliton with $M = 4000$, $\chi = 600$, $h = 0.2$ and $\Delta t = 0.002$

t	IE_1	IE_3	IE_4
8	4.4e−014	2.3e−014	7.4e−013
16	−3.8e−013	−6.0e−013	1.1e−012
24	−8.6e−013	−1.3e−012	1.4e−012
32	−1.1e−012	−1.7e−012	9.1e−013
40	−5.6e−013	−8.7e−013	1.8e−012

numerical results are compared with the methods of CDQ [15], Galerkin (GM) [7], DRK4 [6], and DIMPR [6] and by setting

$$a = -20,\ \ b = 80,\ \ \nu = 1,\ \ \alpha = 1,\ \ e = 2/3,\ \ \delta = 0.5, \tag{4.16}$$

numerical results are compared with the methods of CDQ [15], central difference (CD) [8] and Chebyshev spectral collocation (CSC) [17] in Table 8. In Table 9, we present relative errors of the conserved quantities obtained from the proposed scheme for parameters setting (4.15) with $h = 0.2$ and $\Delta t = 0.002$. Considering parameters setting (4.16), Fig. 19 shows the evolution of single soliton moving to right with velocity $\nu = 1$.

4.2.1 *Interaction of two solitary waves*

Interaction of two solitary waves are studied by using the initial conditions

$$\begin{aligned} u_1(x,0) &= \sum_{j=1}^{2} \sqrt{\frac{2\alpha_j}{1+e}}\,\mathrm{sech}(\sqrt{2\alpha_j}x_j) \\ &\quad \times \exp\left(ii(\nu_j - \delta)x_j\right), \\ u_2(x,0) &= \sum_{j=1}^{2} \sqrt{\frac{2\alpha_j}{1+e}}\,\mathrm{sech}(\sqrt{2\alpha_j}x_j) \\ &\quad \times \exp\left(i(\nu_j + \delta)x_j\right). \end{aligned} \tag{4.17}$$

We choose parameters $x1 = x$, $x2 = x - 25$, $\alpha 1_1 = 1$, $\alpha_2 = 0.5$, $\nu_1 = 1$, $\nu_2 = 0.1$, $\delta = 0.5$, and $e = 2/3$ to compare our results with those in the literature [8, 17]. These parameters give amplitude 1.095445114992280 and 0.7745966692414844 for larger and smaller solitary wave, respectively. Computations are carried out up to time $t = 50$ with time step $\Delta t = 0.002$ and space step $h = 0.2$ on the interval $-20 \le x \le 70$. From the initial conditions (4.17), the solitary wave is propagated rightwards. In this process, the larger and smaller wave unite and separate while preserving their original shapes. Plots of both waves during the interaction from time $t = 0$ to time $t = 50$ are shown in Fig. 20. Three conserved quantities I_1, I_3 and I_4 are presented in Table 10. We used values $M = 4000$, $\chi = 600$, $h = 0.2$, $\Delta t = 0.002$, and domain $[-20, 70]$ to obtain the value of the conserved quantities.

4.2.2 *Interaction of three solitary waves*

Interaction of three solitary waves are studied by using the initial conditions

$$\begin{aligned} u_1(x,0) &= \sum_{j=1}^{3} \sqrt{\frac{2\alpha_j}{1+e}}\,\mathrm{sech}(\sqrt{2\alpha_j}x_j) \\ &\quad \times \exp\left(i(\nu_j - \delta)x_j\right), \\ u_2(x,0) &= \sum_{j=1}^{3} \sqrt{\frac{2\alpha_j}{1+e}}\,\mathrm{sech}(\sqrt{2\alpha_j}x_j) \\ &\quad \times \exp\left(i(\nu_j + \delta)x_j\right). \end{aligned}$$

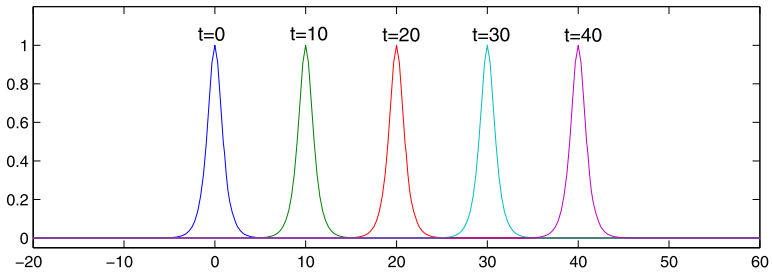

Fig. 19 Motion of single soliton with $M = 4000$, $\chi = 600$, $h = 0.2$, and $\Delta t = 0.002$

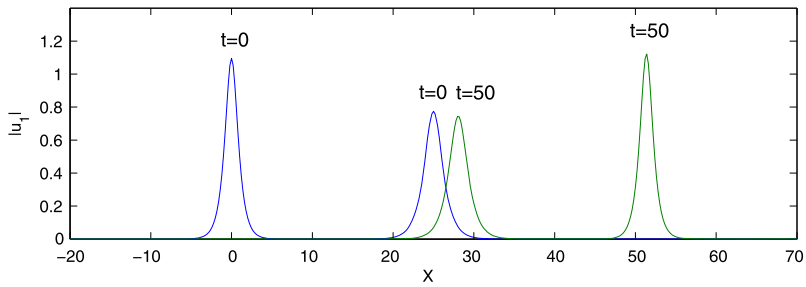

Fig. 20 Interaction of two solitons with $M = 4000$, $\chi = 600$, $h = 0.2$ and $\Delta t = 0.002$

Table 10 Conserved quantities for interaction of two solitons with $M = 4000$, $\chi = 600$, $h = 0.2$, and $\Delta t = 0.002$

t	I_1	I_3	I_4
0	2.8970563	−7.2682	0.9
10	2.8970563	−7.2682	0.9
20	2.8970563	−7.2682	0.9
30	2.8970563	−7.2682	0.8
40	2.8970563	−7.2682	0.8
50	2.8970561	−7.2681	0.8

Table 11 Conserved quantities for interaction of three solitons with $M = 4000$, $\chi = 600$, $h = 0.2$, and $\Delta t = 0.002$

t	I_1	I_3	I_4
0	4.317266	−3.9392	1.5
10	4.317266	−3.9392	1.5
20	4.317266	−3.9392	1.5
30	4.317266	−3.9391	1.3
40	4.317266	−3.9391	1.3
50	4.317265	−3.9388	1.3

We choose the following parameters $x_1 = x$, $x_2 = x - 25$, $x_3 = x - 50$, $\alpha_1 = 1.2$, $\alpha_2 = 0.72$, $\alpha_3 = 0.36$, $\nu_1 = 1.0$, $\nu_2 = 0.1$, $\nu_3 = -1.0$, $\delta = 0.5$, and $e = 2/3$ on domain $[-20, 70]$. We conclude that among the interaction of three solitary waves, two of them are moving in the same direction with different velocities, while the third one is moving in the opposite direction. It is observed that larger, medium, and solitary waves unite and separate while preserving their original shape (see Fig. 21). The values of the three conserved quantities are shown in Table 11.

4.3 Numerical tests of SCNLSEs

For testing elastic collisions, inelastic collisions and fusion properties of two solitons, we consider Eq. (1.3) with initial conditions

$$u_1(x,0) = \sqrt{2}\,\mathrm{sech}\left(x + \frac{D_0}{2}\right)\exp(i\nu_0 x/4),$$

$$u_2(x,0) = \sqrt{2}\,\mathrm{sech}\left(x - \frac{D_0}{2}\right)\exp(-i\nu_0 x/4),$$

where D_0 and ν_0 are constants. First, we consider the elastic collision of two solitons by choosing the parameters $\beta = 1$, $\alpha_1 = 1$, $\alpha_2 = -1/6$, $\gamma = 1$, $\Gamma = 1$, $\nu_0 = 1$, $D_0 = 25$. Figure 22 shows that the proposed scheme simulates the solitary waves well. The two waves emerge without any changes in their shapes. This phenomenon shows that the interaction is elastic. It must be pointed out that the elastic collisions are those from which the newly formed shapes reemerge under deformation.

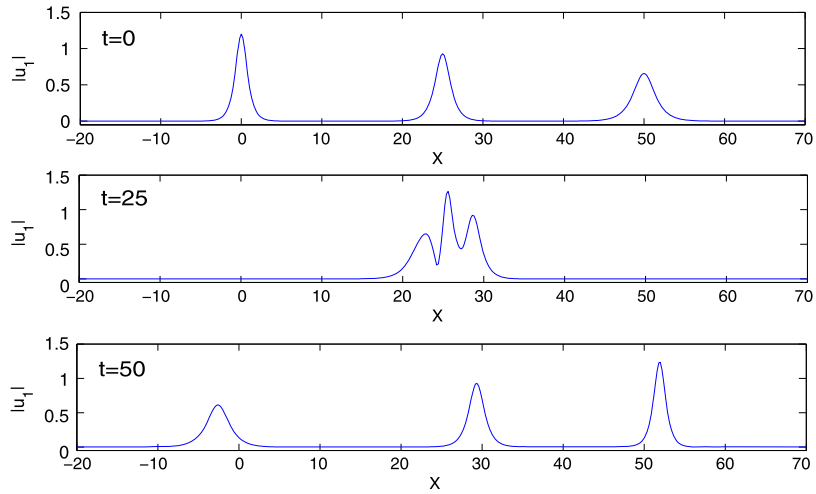

Fig. 21 Interaction of three solitons with $h = 0.02$, $\Delta t = 0.002$, $\chi = 600$, $M = 4000$, and $\delta = 0.5$

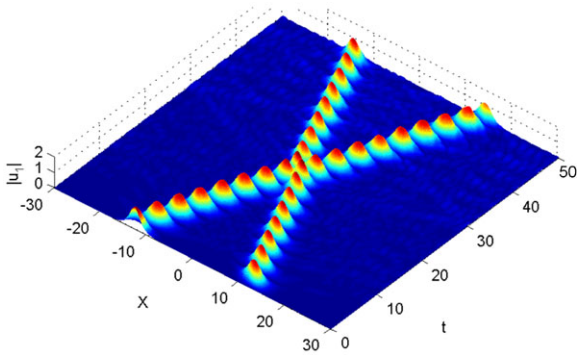

Fig. 22 Elastic collision. $\beta = 1$, $\alpha_1 = 1$, $\alpha_2 = -1/6$, $\gamma = 1$, $\Gamma = 1$, $\nu_0 = 1$, $D_0 = 25$, and $M = 4000$

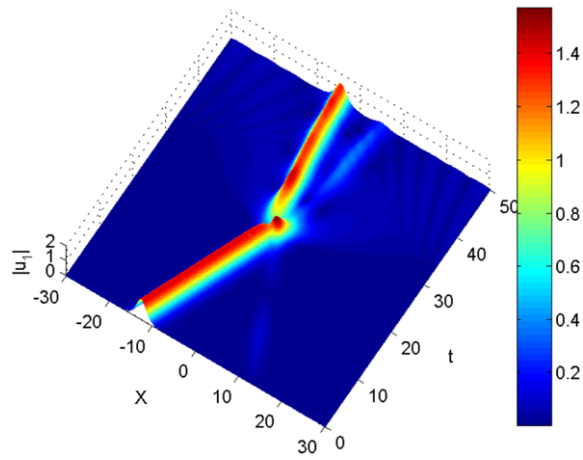

Fig. 23 Inelastic collision. $\beta = 1$, $\alpha_1 = 1$, $\alpha_2 = -1/6$, $\gamma = 1$, $\Gamma = 0.0175$, $\nu_0 = 1$, $D_0 = 25$, and $M = 4000$

Now we consider the inelastic-transitive collision of two solitons. To do so, we choose the parameters $\beta = 1$, $\alpha_1 = 1$, $\alpha_2 = -1/6$, $\gamma = 1$, $\Gamma = 0.0175$, $\nu_0 = 1$, $D_0 = 25$. Figure 23 shows inelastic collision of two solitons. From this figure, we see that, after the interaction, the solitary waves leave dispersive oscillations and their amplitudes are altered. Both waves change their shape and the interaction is inelastic.

We consider now the fusion of two solitons by choosing the parameters $\beta = 1$, $\alpha_1 = 1$, $\alpha_2 = -1/3$, $\gamma = 1$, $\Gamma = 0.0175$, and $\nu_0 = 0.4$, $D_0 = 20$. From Fig. 24, we see that the two solitons collapse into one soliton.

5 Conclusion

Applicability and efficiency of a semidiscrete method based on the newly developed Delta-shaped basis functions have been tested by solving some Schrödinger-type equations. The fourth-order Runge–Kutta method for the time integration of the resulting systems of nonlinear ordinary differential equations has been applied. Some satisfactory numerical simulations such as motion of single solitary wave and double and triple solitary waves, generation of solitary waves using the Maxwellian initial condition, birth of mobile soliton, bound state of solitons, elastic and inelastic collision of two solitons, and fusion of two solitons have been carried out.

Without taking computational costs into account, the first two test problems, the motion of single soliton and interaction of two solitons, have been simulated with more accurate results in comparison with earlier

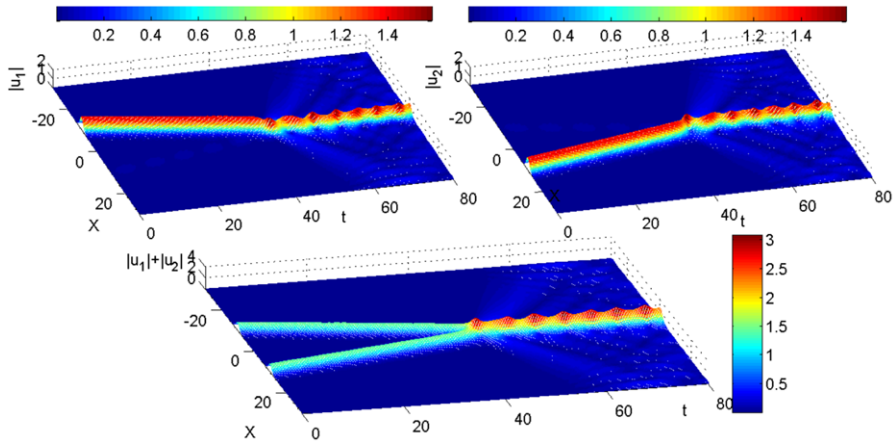

Fig. 24 Fusion of two solitons. $\beta = 1$, $\alpha_1 = 1$, $\alpha_2 = -1/3$, $\gamma = 1$, $\Gamma = 0.0175$ and $\nu_0 = 0.4$, $D_0 = 20$, and $M = 4000$

works and the proposed method can compete very well with the successful method of differential quadrature [10, 11].

Furthermore, the performance of the method has been monitored by computing some conserved quantities. We have found that for almost all of our experiments, invariant quantities are conserved satisfactorily.

Interaction of double and triple solitary waves, generation of solitary waves using the Maxwellian initial condition, birth of mobile soliton, bound state of solitons, and other numerical simulations have been carried out as well as some earlier successful studies.

Finally, our scheme is sensibly conservative and can generate reasonable numerical results.

References

1. Chegini, N.G., Salaripanah, A., Mokhtari, R., Isvand, D.: Numerical solution of the regularized long wave equation using nonpolynomial splines. Nonlinear Dyn. **69**(1–2), 459–471 (2012)
2. Dag, I.: A quartic B-spline finite element method for solving nonlinear Schrödinger equation. Comput. Methods Appl. Mech. Eng. **174**, 247–258 (1999)
3. Delfour, M., Fortin, M., Payne, G.: Finite-difference solutions of non-linear Schrödinger equation. J. Comput. Phys. **44**, 277–288 (1981)
4. Gardner, L.R.T., Gardner, G.A., Zaki, S.I., Sharawi, Z.El.: B-spline finite element studies of the non-linear Schrödinger equation. Comput. Methods Appl. Mech. Eng. **108**, 303–318 (1993)
5. Hon, Y.C., Yang, Z.: Meshless collocation method by Delta-shape basis functions for default barrier model. Eng. Anal. Bound. Elem. **33**, 951–958 (2009)
6. Ismail, M.S.: A fourth-order explicit schemes for the coupled nonlinear Schrödinger equation. Appl. Math. Comput. **196**(1), 273–284 (2008)
7. Ismail, M.S.: Numerical solution of coupled nonlinear Schrödinger equation by Galerkin method. Math. Comput. Simul. **78**(4), 532–547 (2008)
8. Ismail, M.S., Taha, T.R.: Numerical simulation of coupled nonlinear Schrödinger equation. Math. Comput. Simul. **56**(6), 547–562 (2001)
9. Kong, L., Duan, Y., Wang, L., Yin, X., Ma, Y.: Spectral-like resolution compact ADI finite difference method for the multi-dimensional Schrödinger equations. Math. Comput. Model. **55**, 1798–1812 (2012)
10. Korkmaz, A., Dag, I.: A differential quadrature algorithm for simulations of nonlinear Schrödinger equation. Comput. Math. Appl. **56**, 2222–2234 (2008)
11. Korkmaz, A., Dag, I.: A differential quadrature algorithm for nonlinear Schrödinger equation. Nonlinear Dyn. **56**, 69–83 (2009)
12. Miles, J.M.: An envelope soliton problems. SIAM J. Appl. Math. **41**, 227 (1981)
13. Mohebbi, A.: Solitary wave solutions of the nonlinear generalized Pochhammer–Chree and regularized long wave equations. Nonlinear Dyn. **70**(4), 2463–2474 (2012)
14. Mokhtari, R., Mohseni, M.: A meshless method for solving mKdV equation. Comput. Phys. Commun. **183**, 1259–1268 (2012)
15. Mokhtari, R., Samadi Toodar, A., Chegini, N.G.: Numerical simulation of coupled nonlinear Schrödinger equations using the generalized differential quadrature method. Chin. Phys. Lett. **28**(2), 020202 (2011)
16. Mokhtari, R., Ziaratgahi, S.T.: Numerical solution of RLW equation using integrated radial basis functions. Appl. Comput. Math. **10**(3), 428–448 (2011)
17. Rashid, A., Ismail, A.I.: A Chebishev spectral collocation method for the coupled nonlinear Schrödinger equation. Appl. Comput. Math. **9**(9), 104–115 (2010)
18. Reutskiy, S.Y.: A boundary method of Trefftz type for PDEs with scattered data. Eng. Anal. Bound. Elem. **29**, 713–724 (2005)
19. Reutskiy, S.Y.: A meshless method for one-dimensional Stefan problems. Appl. Math. Comput. **217**, 9689–9701 (2011)
20. Tian, H.Y., Reutskiy, S., Chen, C.S.: New basis functions and their applications to PDEs. Int. Conf. Civ. Eng. Sci. **3**(4), 169–175 (2007)

21. Tian, H.Y., Reutskiy, S., Chen, C.S.: A basis function for approximation and the solutions of partial differential equations. Numer. Methods Partial Differ. Equ. **24**, 1018–1036 (2008)
22. Taha, T.R., Ablowitz, M.J.: Analytical and numerical aspects of certain nonlinear evolution equations. II. Numerical, nonlinear Schrödinger equations. J. Comput. Phys. **55**, 203–230 (1984)
23. Whitham, G.B.: Linear and Nonlinear Waves. Wiley-Interscience, New York (1974)
24. Zakharov, V.E., Shabat, A.B.: Exact theory of two dimensional self focusing and one dimensional self waves in nonlinear media. Sov. Phys. JETP **34**, 62 (1972)